Industrial Chemistry & Materials

ROYAL SOCIETY OF CHEMISTRY

REVIEW

View Article Online
View Journal | View Issue

Cite this: *Ind. Chem. Mater.*, 2023, **1**, 582

Recent progress with the application of organic room-temperature phosphorescent materials

Mengxing Ji and Xiang Ma *

Organic materials with room-temperature phosphorescence (RTP) emission have attracted extensive attention owing to their extraordinary properties, including long lifetime, large Stokes shift, and stimuli-responsiveness, and show bright prospects in broad fields. Numerous design strategies, such as creating a rigid environment through crystallization and supramolecular assembly, can be employed to improve the luminescent characteristics of RTP materials by restricting nonradiative transition, enhancing intersystem crossing, and so forth. This review summarizes recent progress with organic room-temperature phosphorescent materials from the perspective of practical applications, including luminescence and display, environmental detection, and bioimaging, and the challenges and prospects will be discussed at the end, which should assist with future research on the application of RTP materials.

Keywords: Room-temperature phosphorescence; OLEDs; Anti-counterfeiting; Environmental detection; Bioimaging.

Received 11th January 2023,
Accepted 3rd March 2023

DOI: 10.1039/d3im00004d

rsc.li/icm

1 Introduction

Organic room-temperature phosphorescent materials are a hot topic with their unique luminescent performance, such as long lifetime and large Stokes shift. According to the luminescence mechanism, the critical steps of phosphorescence emission that are different from fluorescence emission are intersystem crossing (ISC) and radiative transition from the lowest triplet state (T_1) to the ground single state (S_0), which give phosphorescent materials longer emission wavelength and lifetime. Enhancing the ISC process to obtain more triplet excitons and inhibiting nonradiative relaxation pathways by providing rigid environment are effective ways to enhance RTP emission.[1]

Recently, there has been a boom in organic materials with room-temperature phosphorescence (RTP) emission due to their low toxicity and easy preparation compared with metal complexes.[2–8] Meanwhile, there are many diverse strategies to construct RTP materials. Molecular engineering including

Key Laboratory for Advanced Materials, and Feringa Nobel Prize Scientist Joint Research Center, Frontiers Science Center for Materiobiology and Dynamic Chemistry, School of Chemistry and Molecular Engineering, East China University of Science and Technology, Meilong Road 130, Shanghai 200237, P. R. China. E-mail: maxiang@ecust.edu.cn

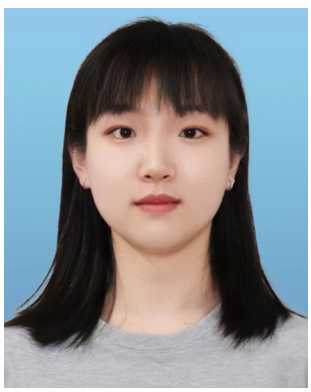

Mengxing Ji

Mengxing Ji obtained her BS from ECUST. She is pursuing her PhD at ECUST under the supervision of Prof. Xiang Ma. Her interests are mainly pure organic RTP materials.

Xiang Ma

Prof. Xiang Ma received his BS from Tianjin University in 2003 and PhD from ECUST in 2008. He has been Professor of Chemistry and Fine Chemicals at ECUST since 2016. His research focuses on organic optoelectronic materials and supramolecules based on dyes. Prof. Ma is a Fellow of the RSC (FRSC) and now serves as Executive Editor of Dyes Pigm. and is on the Colour Index Pigment and Solvent Dyes Technical Board of The Society of Dyers and Colourists (SDC).

introducing heavy atoms (Cl, Br), heteroatoms (N, S, P) and carbonyls[9–11] can directly address the weak spin–orbit coupling (SOC) effect and ultrafast triplet exciton deactivation and then endow pure organic luminophores with long-lived and strong RTP.[12] Crystallization can suppress nonradiative relaxation by restricting intermolecular motions to improve RTP performance.[13–15] Both polymer doping and polymerization can have the same effect, whereby the nonradiative relaxation is inhibited by providing a rigid environment or hydrogen bond network.[16–21] Supramolecular assembly supplies host molecules with a hydrophobic cavity, such as cucurbit[*n*]uril and cyclodextrin, for guest molecule phosphors, which prevents luminophores from being quenched by oxygen and water.[22–26] Host–guest doping of small molecules realizes efficient RTP emission with effective energy transfer by modulating energy levels between them.[27–30] Based on these strategies, the constructed RTP materials are endowed with various luminescent properties in different physical conditions, which makes them exhibit tremendous application value in various fields including light-emitting diodes, anti-counterfeiting, sensors, and bioimaging. In this review, we summarize the recent progress with the application of organic RTP materials constructed by the above strategies.

2 Luminescence and display

2.1 Organic light-emitting diodes

Light-emitting diodes (OLEDs) recently emerged and exhibit excellent performance in display screens, and the search and development for high external quantum efficiency (EQE) and high-performance OLEDs is still a hot topic. The internal quantum efficiency (IQE) of emitting materials is essential to improve the device EQE, while only 25% of single excitons can be utilized to emit light in fluorescent materials; therefore, the harvesting of both single and triplet excitons to achieve a theoretical IQE of 100% makes phosphorescent materials attractive.[31–35] Since Ceroni *et al.* realized the application of pure organic RTP materials in OLEDs for the first time in 2013,[36] OLEDs based on them have made great progress.

In 2019, Zhang and coworkers designed a series of single molecules with RTP emission through introducing different substituents onto biscarbazole (BCZ) (Fig. 1), which possessed aggregation-induced emission (AIE) characteristics so that these molecules could exhibit phosphorescence with a quantum yield of up to 64% in the solid state.[37] Therefore, the single molecular materials were applied in OLEDs as emitting layers in a non-doped way, and the acetophenone-modified BCZ realized an EQE of 5.8%.

In 2021, Ding *et al.* constructed a pure organic RTP polymer named P(DMPAc-O-TPTrz) with a donor–oxygen–acceptor (D–O–A) geometry (Fig. 2a) and applied it towards polymer light-emitting diodes (PLEDs).[38] Different from the conventional donor–acceptor geometry, the inserted oxygen atom in the D–O–A geometry took effect in two aspects: one

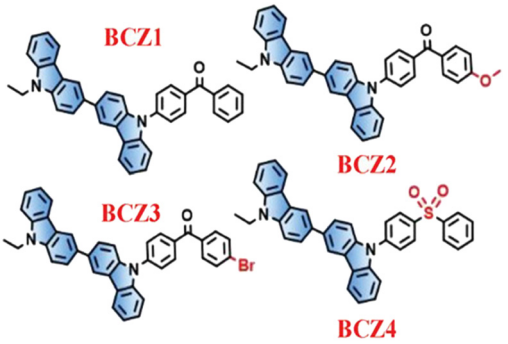

Fig. 1 Chemical structures of AIE (BCZ1–3) or aggregation-induced-emission-enhancement (AIEE) (BCZ4)-type molecules (reproduced with permission from ref. 37. Copyright 2019, WILEY-VCH Verlag GmbH & Co. KGaA, Weinheim).

is to decrease hole–electron orbital overlap to suppress the charge-transfer fluorescence, and the other is to strengthen the spin–orbital coupling effect, which facilitated ISC to generate RTP. P(DMPAc-O-TPTrz) displayed RTP emission with a wavelength of 486 nm and photoluminescence quantum yield (PLQY) of 21.4% in the solid state due to the AIE characteristic. The PLEDs were prepared with mCP doping 15 wt% P(DMPAc-O-TPTrz) as the emitter layer and an optimized EQE of 9.7% was achieved along with CIE coordinates of (0.27, 0.41).

In the same year, Data *et al.* synthesized a heavy-atom-free single molecule named SiAZ, whose emission channels could switch between thermally activated delayed fluorescence (TADF) and RTP with different host matrixes (Fig. 2b), and

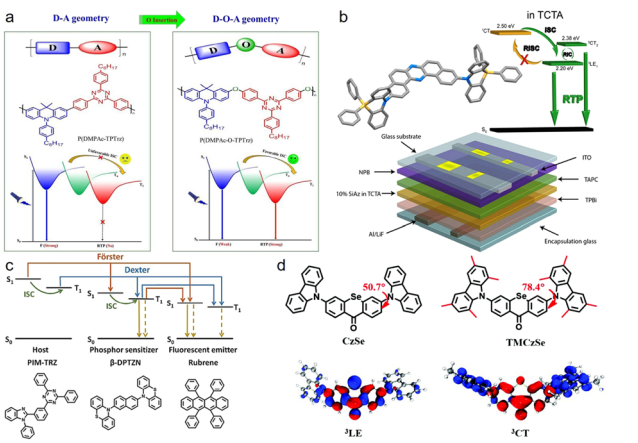

Fig. 2 (a) Molecular design from fluorescence polymers with a D–A geometry to pure organic RTP polymers with a D–O–A geometry (reproduced with permission from ref. 38. Copyright 2020, Wiley-VCH GmbH). (b) Illustration of OLED device with 1% w/w SiAz in TCTA (reproduced with permission from ref. 39. Copyright 2021, American Chemical Society). (c) Illustration of phosphor-sensitizing mechanism and molecular structures of PIM-TRZ, β-DPTZN, rubrene used in devices (reproduced with permission from ref. 40. Copyright 2021 Wiley-VCH GmbH). (d) Molecular structures of CzSe and TMCzSe and the twisting angles between the donor and acceptor units; hole and electron distributions of T_1 for CzSe and TMCzSe (reproduced with permission from ref. 41. Copyright 2022, Royal Society of Chemistry).

successfully obtained heavy-atom-free RTP organic OLEDs.[39] The three host matrixes including Zeonex, bis[2-(diphenylphosphino)phenyl]ether oxide (DPEPO) and tris(4-carbazoyl-9-ylphenyl)amine (TCTA) could tune the singlet and triplet excited state energies subtly due to their polarity effect. Among them, the material based on TCTA had only RTP emission, and the corresponding OLEDs achieved an EQE of 4.06% and luminance of 22 561 cd m^{-2}.

Though RTP-based OLEDs have attracted tremendous attention due to various properties, the low PLQYs in the thin film state restricted the development of highly efficient OLEDs. Wang *et al.* innovatively designed a purely organic phosphor-sensitizing fluorescence emitter and fabricated highly efficient OLEDs with EQE up to 15.7% (Fig. 2c).[40] This is a new strategy for achieving electroluminescence with 100% IQE. Benzimidazole–triazine molecules (PIM–TRZ), 2,6-di(phenothiazinyl)naphthalene (b-DPTZN), and 5,6,11,12-tetraphenylnaphthacene (rubrene) were selected as the host, phosphorescent sensitizer, and fluorescent emitter, respectively. A facile Förster energy transfer occurred from the phosphor sensitizer to rubrene in the system and the PIM–TRZ host with RTP feature also played a key role in the process. Therefore, the combination of these three compounds resulted in the construction of cost-effective high-performance OLEDs.

The short lifetime is also significant for obtaining highly efficient OLEDs in addition to high PLQYs. In 2022, Wang *et al.* fabricated two twisted donor–acceptor–donor (D–A–D) type organic emitters named CzSe and TMCzSe, which had different twist angles between the D and A units to modulate the lowest triplet excited state from locally excited triplet states (^{3}LE) to triplet charge-transfer states (^{3}CT) (Fig. 2d).[41] CzSe only had RTP emission with ^{3}LE as the T_1 state while TMCzSe possessed both RTP and TADF with ^{3}CT featuring triplet excited states, which resulted in the higher PLQYs and shorter lifetime for TMCzSe compared to CzSe. Furthermore, the purely RTP-based OLEDs with CzSe achieved a high EQE of 8.9% and the EQE of OLEDs based on TMCzSe reached 25.5% owing to the higher PLQY.

2.2 Anti-counterfeiting and data encryption

Anti-counterfeiting or data encryption based on RTP materials is a common and popular application due to the UV light irradiation characteristic and different lifetimes. RTP materials constructed by various strategies have been applied in this field,[42–46] and herein some interesting recent work involving multiple anti-counterfeiting or data encryption based on time resolution or chemical response is summarized briefly.

In addition to the simple anti-counterfeiting and data encryption based on the on–off switching of UV light,[47–50] the different lifetimes create a feasible way to realize multiple anti-counterfeiting or data encryption by utilizing the time resolution technique. In 2020, An *et al.* adopted molecular engineering whereby a methylene linker was introduced to bridge the carbazole and halogenated phenyl ring to construct RTP phosphors CzBX (X = Cl, Br) (Fig. 3a).[51] Compared to the donor–acceptor molecule CzPX, the sp^3 methylene linkers could induce tetrahedron-like structures that could restrain the nonradiative decay channel and weaken the impact of the heavy-atom effect, and thus CzBX exhibited increased phosphorescence efficiency and longer lifetime. With the gradually decreased lifetimes of CzBCl, CzBBr, and CzPBr, a multi-element pattern appeared with different information so that multiple anti-counterfeiting and data encryption were achieved.

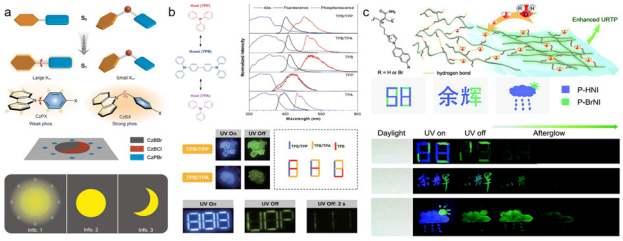

Fig. 3 (a) Illustration of the design concept and molecular structures of CzPX and CzBX (X = Cl, Br); three encrypted information patterns using CzBBr, CzBCl, and CzPBr (reproduced with permission from ref. 51. Copyright 2020, Wiley-VCH GmbH). (b) The chemical structures of host and guest molecules and relative optical spectra; demonstration of triple anti-counterfeiting using the TPB/TPP, TPB/TPA, and TPB crystals (reproduced with permission from ref. 52. Copyright 2021, Science China Press and Springer-Verlag GmbH Germany, part of Springer Nature). (c) Illustration of enhanced RTP with a water-induced hydrogen bridge network; demonstration of patterns written in P-BrNI and P-HNI inks (reproduced with permission from ref. 53. Copyright 2021, Royal Society of Chemistry).

The host–guest doping strategy is often employed to design ultralong organic RTP materials. In 2021, Qin *et al.* chose *N*,*N*,*N*′,*N*′-tetraphenylbenzidine (TPB) as a guest with triphenylamine (TPA) and triphenylphosphine (TPP) as hosts to construct RTP systems (Fig. 3b).[52] These compounds are commercially available. TPB alone emits a very weak phosphorescence with a short lifetime, while the host–guest doping systems, TPB/TPP and TPB/TPA, showed long RTP lifetimes of 362 and 199 ms, respectively. In the RTP systems, the host molecules not only provide a rigid environment to suppress nonradiative decay of the guest, but also facilitate phosphorescence of the guest through Förster resonance energy transfer (FRET). Similarly, an anti-counterfeiting pattern "888" was designed with three compounds and different figures emerged due to various lifetimes of afterglow.

Copolymerizing phosphors with acrylamide is an impressive strategy to afford an efficient RTP material, because the rigid environment and hydrogen bond network supplied by polyacrylamide can inhibit the nonradiative decay process. In 2021, Ma *et al.* used this strategy to fabricate pure organic URTP copolymers (P-BrNI and P-HNI), and, moreover, enhanced their RTP lifetimes and quantum yields through evaporating aqueous copolymer solution to form copolymer films with water molecules as a hydrogen bridge (Fig. 3c).[53] Due to the distinguishable phosphorescence lifetimes of

P-BrNI and P-HNI, the two materials were applied as a security ink and realized time-resolved multiple information encryption.

The chemical-responsive RTP is also a feasible means to realize multiple anti-counterfeiting. In 2021, Li *et al.* developed a host–guest doping system and realized anti-counterfeiting printings to commercialize RTP materials.[54] In this work, triphenylphosphine oxide ($OPph_3$) acted as a host and a series of benzo(dibenzo)phenothiazine dioxide derivatives (Pph, BPph, and DBPph) was chosen as guests firstly (Fig. 4a). In these host–guest doping systems energy transfer would occur from host to guest, but they displayed different phosphorescence efficiencies and lifetimes due to different abilities of the guest molecules in terms of energy transfer and triplet emission. Besides, the pyridine-substituted guest molecules (Ppy, BPpy, and DBPpy) exhibited similar photophysical properties to the former guest molecules, and the new host–guest doping systems could respond to proton acid, showing reversible stimulus-responsive RTP emission. Therefore, the BPpy/$OPPh_3$ system was used as a security ink and stylus/thermal printing paper, and then realized multiple anti-counterfeiting under the function of acid and NH_3.

In the same year, Ma *et al.* constructed circularly polarized RTP materials (R/S-BPNaP) by radical binary copolymerization of acrylamide and chiral binaphthyl derivates (Fig. 4b).[55] Choosing R-BPNaP as an example, when inducing HBr into the copolymer system, the obtained R-BPHP exhibited increased RTP emission intensity but decreased lifetime because of the intermolecular heavy-atom effect, which showed the acid–alkali responsive property. The longer lifetime of R-BPNaP protected the number "5" hidden in "8" written with R-BPHP.

In 2022, Ma *et al.* reported another circularly polarized phosphorescent material by homogeneously dispersing phosphorescent chiral helical substituted polyacetylenes into a poly(methyl methacrylate) (PMMA) matrix, and realized a time-informed anti-counterfeiting application with photoprogrammability.[56] The chiral polymer was constructed by copolymerizing chiral 4-isobutylphenyl-*N*-propanamide derivative (phNA) and the RTP chromophore 4-bromo-1,8-naphthalimide derivative (BrNpA) and the rigid matrix PMMA was used to enhance the RTP emission. The p(phNA$_7$-BrNpA$_3$)-PMMA film exhibited time-dependent tunable RTP intensity because of the consumption of oxygen in the PMMA matrix under continuous UV irradiation. Based on this characteristic, the different copolymerization molar ratios of the materials were utilized to fabricate lampshades and form a lamp panel that could detect different digital patterns on different time scales. Besides, the p(phNA$_7$BrNpA$_3$)-PMMA film could also realize anti-counterfeiting application involving CPL signal.

2.3 Others

In addition to the applications in OLEDs, anti-counterfeiting, and data encryption, the unique luminescence performance of RTP materials also makes them useful in printing and visualization of latent fingerprints, two rare but meaningful applications.

In 2019, Zhao *et al.* designed pure organic RTP materials based on (4-(9*H*-carbazol-9-yl)butyl) triphenylphosphonium with different halide anions, named CBTP-Cl, CBTP-Br, and CBTP-I, whose luminescence could be tuned by changing the halide anions (Cl^-, Br^-, and I^-) (Fig. 5a).[57] Tunable emission

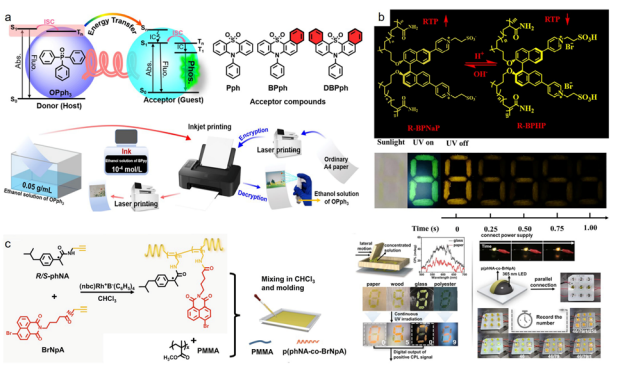

Fig. 4 (a) Energy transfer between donor (host) and acceptor (guest) and molecular structures of acceptors; the production of anti-counterfeiting marks using inkjet printing (reproduced with permission from ref. 54. Copyright 2021, Wiley-VCH GmbH). (b) Illustration of acid–alkali responsive structure of R/S-BPNaP and R/S-BPHP. Photographs of number "8" written using aqueous R-BPHP and "5" written using aqueous R-BPNaP on the same number "8" (reproduced with permission from ref. 55. Copyright 2021, Elsevier B.V). (c) Schematic illustration of the structure and preparation of the p(phNA-*co*-BrNpA)-PMMA film and its anti-counterfeiting application (reproduced with permission from ref. 56. Copyright 2022, Springer Nature).

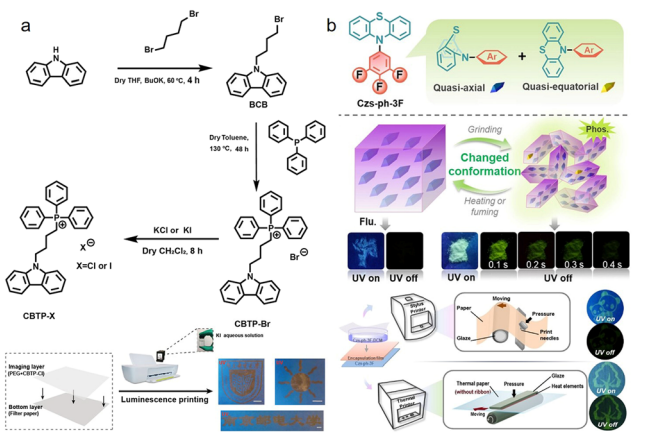

Fig. 5 (a) Synthetic routes for CBTP-Cl, CBTP-Br, and CBTP-I; the luminescent images printed on the prepared paper using a commercial inkjet printer equipped with an ink cartridge filled with KI aqueous solution (reproduced with permission from ref. 57. Copyright 2019, WILEY-VCH Verlag GmbH & Co. KGaA, Weinheim). (b) The molecular structure and two possible conformations of CzS-ph-3F and a proposed diagram for the stimulus-responsive RTP effect based on conformational change; application of stylus printing and thermal printing (reproduced with permission from ref. 58. Copyright 2021, Wiley-VCH GmbH).

colors of the polymer film containing CBTP-Cl could be achieved by introducing various ratios of potassium iodide (KI). The external heavy-atom effect had a key influence in the process. Therefore, based on the special function between the polymer film containing CBTP-Cl and KI, the PEG matrix containing CBTP-Cl was made into a paper substrate and information was recorded successfully using a commercial inkjet printer with KI as the ink.

In 2021, Li and coworkers constructed a purely organic force-induced turn-on RTP material named Czs-ph-3F, which comprised electron donor phenothiazine and acceptor trifluorobenzene (Fig. 5b).[58] The conformation of partial Czs-ph-3F molecules would transfer from quasi-axial (ax) to quasi-equatorial (eq) after grinding so that a self-doping system formed and emitted green RTP. The transformation of molecular packing has a significant effect on photoelectronic properties.[59,60] The RTP emission would disappear under heating or fuming. Based on this, the typing paper was made from transparent encapsulation film with Czs-ph-3F layer having no RTP and a stylus printer was used to print a pattern successfully with force stimulus but no clear afterglow was observed, while the pattern printed using the thermal printer gave a clearer afterglow under the dual actions of heating and pressure.

Fingerprints contain personal information, the detection of which is significant in forensic investigations and identification. In 2019, Ma *et al.* designed two RTP compounds (BrNpA-bisUPy and BrBA-bisUPy) by attaching ureidopyrimidinone (UPy) units to the ends of two phosphors, BrNpA and BrBA (Fig. 6a).[61] Solid films of BrNpA-bisUPy and BrBA-bisUPy exhibited fluorescence emissions together with RTP at 587 and 490 nm, resulting in orange and cyan emissions, respectively. Moreover, the UPy moieties could form quadruple hydrogen bonding to protect phosphors from quenching by oxygen and water so that the RTP materials were insensitive to them. On account of the hydrophobicity, BrBA-bisUPy would adhere to the ridges of sebaceous fingerprints with simple experimental operation, and the latent fingerprints were visualized with cyan emission irradiated by UV light.

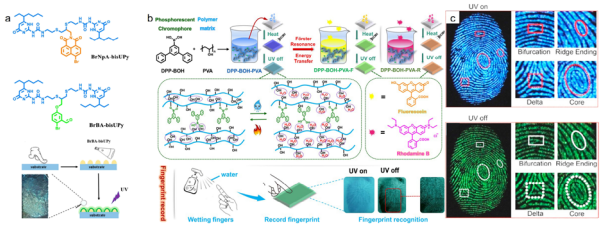

Fig. 6 (a) Chemical structures of BrNpA-bisUPy and BrBA-bisUPy and preparation of a LFP and a photograph of the LFP under UV light (reproduced with permission from ref. 61. Copyright 2019, American Chemical Society). (b) Schematic illustration of the synthetic process for three target products and changes in intermolecular interactions under heating or water stimulus and the application for fingerprint recording (reproduced with permission from ref. 62. Copyright 2022, Springer Nature). (c) Photographs of a fingerprint developed by CPs@silica powder on black marble under 365 nm UV light on and off with regional specific details (reproduced with permission from ref. 64. Copyright 2022, Elsevier B.V).

In 2022, Li *et al.* designed a polymer film (DPP-BOH-PVA) by bonding arylboronic acid into poly(vinylalcohol) (PVA) and applied it in various fields, one of which was fingerprint recording (Fig. 6b).[62] The polymer exhibited excellent RTP properties with a lifetime of 2.43 s and a phosphorescence quantum yield of 7.51%. RTP materials often respond to external stimuli, which makes them widely applied.[63] The rigid hydrogen bond network brought by PVA could be destroyed by water, so the RTP emission of the polymer film was sensitive to the stimuli of water and heat. Based on the water-sensitive RTP emission property, the fingerprint would be recorded in the desiccative DPP-BOH-PVA film with the wet protruding parts and untouched recessed position of the fingerprint.

In the same year, Shao *et al.* studied in great depth latent fingerprint imaging with carbonized polymers (CPs) dispersed in silica gel medium.[64] The CPs were synthesized by one-step pyrolysis using ethylenediamine and phosphoric acid as precursors and exhibited green RTP emission. To realize application in visualizing latent fingerprints, the CPs were dispersed in silica gel to form CPs@silica powder. The fingerprint exhibited both fluorescent and phosphorescent images, and ridges, furrows, and even regional details of the whole fingerprint could be distinguished (Fig. 6c). Especially, the high-resolved phosphorescent fingerprints on background fluorescence substrates could still be observed when UV light was off. CPs@silica powder displayed outstanding application value in visualization of latent fingerprints.

3 Environmental detection

It is well known that there are many factors affecting the luminescent properties of RTP materials, such as oxygen and temperature, and thus chemical sensors based on RTP are also an essential research direction and can produce practical applications in environmental detection.

The spin triplet characteristic of ground state oxygen means that O_2 can quench triplet excitons of RTP materials easily, which also makes RTP materials ideal candidates for detecting O_2.[65,66] Usually, the decreasing phosphorescent intensity and lifetime can both be utilized to realize quantitative detection of oxygen.

In 2014, Ermolina *et al.* realized oxygen concentration detection in the range of 0 to 100% based on the phosphorescent intensity of diiodine-substituted boron dipyrromethene (I_2BODIPY) dye in Ar and O_2 (Fig. 7a).[67] The I_2BODIPY was incorporated in a methylcellulose matrix, which possessed a relatively high oxygen permeability and good optical properties, and then the dye-impregnated matrix was applied to detect O_2. Moreover, the concentration of dye molecules influenced the oxygen detection limit to some extent, and the ratio of intensities in ambient conditions with

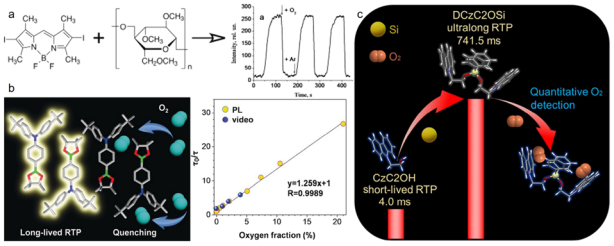

Fig. 7 (a) O_2 sensor based on phosphor I_2BODIPY in the range of 0–100% (reproduced with permission from ref. 67. Copyright 2014, Elsevier B.V). (b) Illustration of RTP emission quenched by O_2 and plots of τ_0/τ against oxygen fraction for TBBU-doped film (reproduced with permission from ref. 69. Copyright 2019 Wiley-VCH Verlag GmbH & Co. KGaA, Weinheim). (c) Illustration of quantitative detection of O_2 for DCzC2OSi-doped film (reproduced with permission from ref. 70. Copyright 2021, Chinese Chemical Society).

different concentrations of oxygen was linear to the oxygen concentration when the concentration of active substance was 10^{-3} M. The dye-based sensor showed high selectivity and fast response to oxygen. Later, in 2022, Wang *et al.* adopted isomer engineering to design three donor–acceptor isomers that were doped in polystyrene films, and two among them could exhibit RTP emission, and likewise their linear relationship between phosphorescent intensity and O_2 concentration allowed quantitative detection of oxygen from 0 to 2.1×10^5 ppm.[68] In 2019, Liang *et al.* constructed a molecule named TBBU with a D–π–A geometry and in the TBBU-doped film the ratio of the initial and decreasing lifetimes caused by O_2 is linearly relative to the oxygen fraction, which was employed for quantitative oxygen detection (Fig. 7b).[69] The TBBU crystals were different from conventional RTP crystals in packing manners, with molecules aligned in a head-to-tail manner with intermolecular aromatic rings arranged side-by-side, so that the oxygen molecules were allowed to disperse. Therefore, the TBBU-doped film was fabricated to detect oxygen and with increasing oxygen fraction from 0 to 21 vol% the change in color and lifetime supplied the basis for quantitative analysis of O_2. Besides, a feasible and convenient method for detecting the oxygen fraction was realized by combing the experimental results with electronic equipment.

Similarly, in 2022, Wu *et al.* synthesized a silicon-based crystal with RTP emission by bridging two carbazoles with ethoxysilane (DCzC2OSi) for oxygen sensing (Fig. 7c).[70] The DCzC2OSi crystals could form oxygen diffusion channels because silicon and ethoxy groups would increase the distance among carbazoles. Likewise, a linear relationship was achieved between the ratio of the lifetime and the concentration of oxygen in the DCzC2OSi-doped film, and the lifetime-based oxygen sensor showed a high Stern–Volmer constant of about 5.308 kPa^{-1} and an oxygen quenching efficiency of 99.1% when the oxygen concentration was up to 21%.

Temperature is also a significant external environmental factor that affects RTP emission because high temperature will enhance nonradiative transition, and thus corresponding RTP materials are developed for temperature sensing. In 2021, Ma *et al.* fabricated phosphorescent fluid materials that were applied for quantitative analysis of temperature ranging from 293 K to 353 K and visualizing the heat distribution of irregular surfaces.[71] These flowable materials were constructed from two organic acids (malic acid and citric acid), β-CD and three organic dyes (7-chlorothiochroman-4-one, 1-bromonaphthalene, and *N*-propyl-4-bromo-1,8-naphthalimide), and the fluid material (RMM) composed of *N*-propyl-4-bromo-1,8-naphthalimide, malic acid (MM), and β-CD was utilized for temperature sensing research (Fig. 8a). The functional relationship between the correlated color temperature index mired value obtained from the CIE coordination and temperature was fitted and used to estimate the environmental temperature. Besides, the qualitative observation of temperature in various surfaces could be achieved due to the flowability, viscosity, and sensitivity to temperature of RMM.

In 2022, Ji *et al.* developed a supramolecular architecture (MP-G crystals) with RTP emission by assembling 4-(methoxycarbonyl)phenyl-boronic acid (MP) with water and realized colorimetric detection of temperature in the range of 300 to 230 K based on crystalline transformation (Fig. 8b).[72] The water in the MP-G crystals could form hydrogen bonds to help enhance the RTP emission and the phosphorescence quantum yield increased from 0.5% to 12.8% and the lifetime increased from 72 ms to 880 ms compared to MP crystals. When the temperature decreased from 300 to 230 K, the color changed from green to blue and there was a linear relationship with temperature in CIE coordinates, together with crystalline transforming from MP-G to MP-B. Therefore,

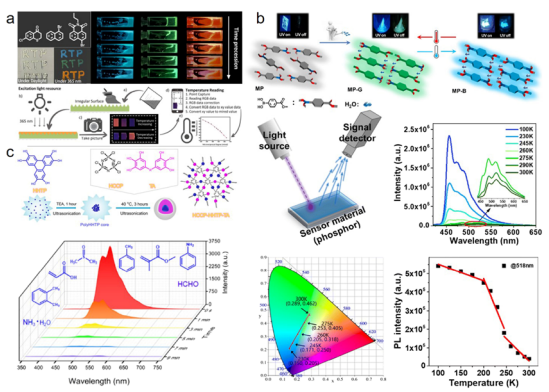

Fig. 8 (a) Structure of phosphors used to construct flowable materials and their photographs; illustration of temperature quantitative detection process by RMM (reproduced with permission from ref. 71. Copyright 2021, Wiley-VCH GmbH). (b) Illustration of the luminescence mechanism of the designed crystals and assembly architecture and application for temperature sensing (reproduced with permission from ref. 72. Copyright 2022, Royal Society of Chemistry). (c) Synthetic route and cross-linked structures of nanospheres and competition experiments with HCCP-HHTP-TA-doped films for the detection of anisole in the presence of other VOCs (reproduced with permission from ref. 73. Copyright 2022, American Chemical Society).

MP-G crystals revealed potential value for low-temperature sensing applications.

The quenching effect of small organic molecules on RTP emission makes chemical sensors based on RTP materials possible. In 2022, Yang *et al.* constructed cross-linked polyphosphazene nanospheres (HCCP-HHTP-TA) with strong RTP and the RTP material exhibited highly selective recognition toward anisole (a volatile organic compound, VOC) when doped into the PVA matrix (Fig. 8c).[73] The multiple carbonyl groups (C═O), heteroatoms (N and P), and heavy atoms (Cl) in HCCP-HHTP-TA and the rigidification effect of the PVA matrix had a great influence on the RTP performance. In the VOC detection experiment, the phosphorescence intensity of the film at 482 nm was quenched completely by anisole, but only a little by other VOCs, showing good selectivity. The Stern–Volmer plot for anisole also showed a good linear correlation that could be used to quantify the anisole concentration. Besides, the anisole sensing mechanism was confirmed to be Dexter energy transfer due to the smaller ΔE_{ST} value between the S_1 of HCCP-HHTP-TA and the T_1 of anisole than that of HCCP-HHTP-TA-doped films.

4 Bioimaging

Optical imaging plays a significant role in biomedical and clinical research,[74,75] where various luminescence types are developed and applied, including fluorescence, delayed fluorescence, phosphorescence, and so on.[76–78] Among them, great progress has been made recently with bioimaging based on pure room-temperature phosphorescence. Compared with fluorescence, RTP has a longer lifetime at longer wavelength, which is beneficial for eliminating fluorescence background interference and scattered light and gaining a higher signal-to-noise ratio (SBR).[79,80] Here we introduce recent research findings from aspects of supramolecular and small molecular systems.

4.1 Supramolecular system

Though RTP materials have many advantages in bioimaging, the nonradiative decay and quenchers in aqueous solution greatly hamper their practical application. In 2020, Ma *et al.* reported visible-light-excited RTP in aqueous solution by using a supramolecular host–guest assembly strategy and utilized it in cell imaging for the first time.[81] This work constructed a TBP-CB[8] assembly system including a heavy-atom-modified molecule (triazine derivative, TBP) with the supramolecular host molecule cucurbit[8]uril (CB[8]) (Fig. 9a), where the cavity of CB[8] can protect TBP from quenchers in solution and suppress the molecular motion, resulting in a long lifetime of 0.190 ms with a 2 : 2 quaternary complex structure in aqueous solution. The assembly system was applied in HeLa cell imaging and the results displayed bright-yellow phosphorescence with excitation wavelength up to 405 nm.

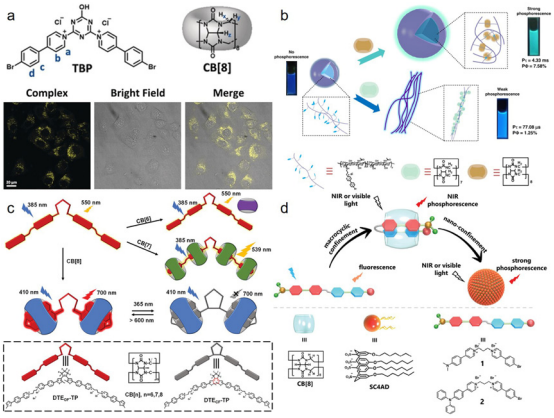

Fig. 9 (a) Chemical structures of TBP and CB[8] and confocal microscopic images of HeLa cells. (reproduced with permission from ref. 81. Copyright 2019, Wiley-VCH Verlag GmbH & Co. KGaA, Weinheim). (b) The construction and behavior of CBs/HA-BrBP supramolecular pseudorotaxane polymers in aqueous solution (reproduced with permission from ref. 82. Copyright 2020, Springer Nature). (c) Schematic illustration and chemical structures of the photo-controlled NIR phosphorescence of DTE-TP/CB[8] (reproduced with permission from ref. 83. Copyright 2022, Wiley-VCH GmbH). (d) Schematic illustration of the formation of supramolecular assembly 1/CB[8]/SC4AD (reproduced with permission from ref. 84. Copyright 2022, Wiley-VCH GmbH).

Subsequently, Liu *et al.* combined host molecules cucurbit[*n*]uril (CB[7], CB[8]) with polymer hyaluronic acid (HA) conjugated to a 4-(4-bromophenyl)pyridin-1-ium bromide (BrBP) phosphor by means of host–guest interactions, creating two water-soluble ultralong organic room-temperature phosphorescent supramolecular polymers (Fig. 9b).[82] Both CB[7]/HA-BrBP and CB[8]/HA-BrBP showed RTP emission at 500 nm, while the latter had better optical properties than the former with a lifetime of 4.33 ms and a quantum yield of 7.58%, benefiting from the stronger host–guest interactions and hydrogen bond. Therefore, CB[8]/HA-BrBP was applied for tumor cell imaging. Three types of cancer cells including A549, HeLa, and KYSE-150 were incubated with CB[8]/HA-BrBP, which emitted strong green phosphorescence and overlapped with the mitochondrion marker MitoTracker Red entirely. In addition, the standard CCK-8 assay results indicated that CB[8]/HA-BrBP had low cytotoxicity. Furthermore, through adding up-conversion nanoparticles (UCNPs) to the supramolecular polymer, the new system of UCNPs + CB[8]/HA-BrBP could realize phosphorescence imaging towards cancer cells excited by near-infrared light (980 nm) and visible light (488 nm), exhibiting excellent application value.

Later, Liu and coworkers carried out further studies in bioimaging based on supramolecular systems and made great progress. In 2022, they constructed a macrocycle-confined purely organic RTP supramolecular assembly by combining diarylethene phenylpyridinium derivative (DTE-TP) with CB[8] that could emit efficient NIR phosphorescence at 700 nm (Fig. 9c).[83] The guest molecule DTE-TP was folded in the cavity of CB[8], and finally enhanced the intramolecular charge-transfer interactions. Furthermore, the DTE-TP/CB[8] could reversibly transfer between the open-

form isomer (DTE_{OF}-TP) and the closed-form isomer (DTE_{CF}-TP) with irradiation of UV light (365 nm) and visible light (>600 nm). Therefore, DTE-TP/CB[8] was used successfully to realize photo-controlled NIR phosphorescence lysosome-targeted cell imaging with the results indicating that A549 cells (human lung cancer cell line) emitted NIR phosphorescence at 650–750 nm and overlapped well with the lysosome marker LysoTracker Green.

In the same year, the group reported three works using a similar strategy of multilevel supramolecular assembly but obtaining different results. The first work obtained a two-stage confinement supramolecular assembly showing two photons excited by near-infrared phosphorescence (Fig. 9d).[84] The host–guest complex combined a guest molecule possessing a D–A structure with the host molecule CB[8] which could promote intramolecular charge-transfer by stacking the donor moiety and acceptor moiety in the cavity, and achieved NIR phosphorescent emission up to 800 nm with the two-photon absorption. The second assembly with amphiphilic macrocycle sulfonatocalix[4]arene (SC4AD) was beneficial for enhancing the phosphorescence intensity and realizing cell imaging with the formation of nanoparticles. The final supramolecular assembly achieved outstanding two-photon cell imaging performance with a higher signal-to-noise ratio compared to the one-photon imaging; in addition, the product was applied in tissue and *in vivo* imaging and exhibited a bright NIR phosphorescence signal. The second work constructed a purely organic supramolecular assembly with CB[8], 4-bromophenyl pyridine salt having an alkyl chain length of 6 or 12 carbon atoms and sulfonated β-cyclodextrin, which exhibited three-photon absorption and phosphorescence emission at 510 nm.[85] The third work reported a noncovalent macrocycle-confined supramolecular assembly composed of a dodecyl-chain-bridged 6-bromoisoquinoline derivative, CB[7] and β-cyclodextrin-grafted hyaluronic acid which could also achieve long-lived NIR emission and was applied in targeted imaging of cancer cells.[86]

4.2 Small molecular systems

Great developments have been made with purely organic RTP materials constructed from small molecules in recent years,[87–89] while the triplet state of small molecule is prone to nonradiative decay, causing the decrease of lifetime or even quenching of RTP, which limits the development of small molecular RTP materials in bioimaging. In 2017, Pu *et al.* proposed a top-down nanoparticle formulation to synthesize water-soluble organic nanoparticles with ultralong phosphorescence for *in vivo* afterglow imaging for the first time,[90] and thus extraordinary achievements have been made with RTP materials based on small molecules.

In 2021, Li and coworkers reported a doped system by integrating an RTP host and an RTP guest, which was encapsulated by the biocompatible amphiphilic copolymer PEG-*b*-PPG-*b*-PEG (F127) to form nanocrystals, which could emit persistent phosphorescence for 25 min in aqueous solution.[91] Two phenothiazine derivatives M-CH_3 (CzS–CH_3 and CzS–C_2H_5)

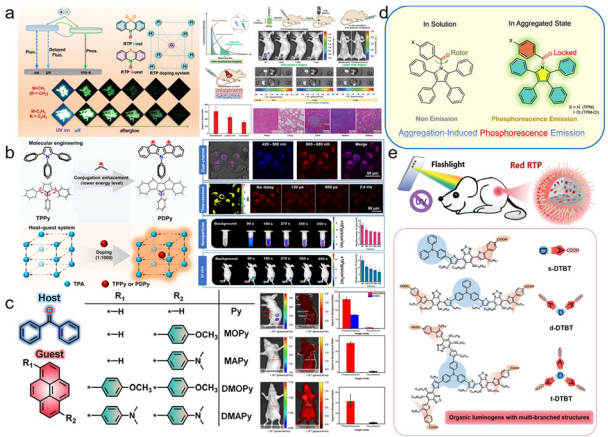

Fig. 10 (a) Illustration of the RTP behaviors of the host–guest doping systems based on M-CH_3 and M-C_2H_5 and application for bioimaging (reproduced with permission from ref. 91. Copyright 2021, Wiley-VCH GmbH). (b) Design concept for highly efficient red-phosphorescence material through molecular engineering and host–guest system and bioimaging application based on the host–guest system (reproduced with permission from ref. 92. Copyright 2021, Chinese Chemical Society). (c) Molecular structures of the guest and host molecules and applications in intravital phosphorescence imaging (reproduced with permission from ref. 93. Copyright 2022, Springer Nature). (d) The molecular design strategy for the AIP compounds (reproduced with permission from ref. 94. Copyright 2022, Springer Nature). (e) Schematic illustration of visible-light-excited afterglow bioimaging with red room-temperature phosphorescence emission and molecular structures of organic luminogens s-DTBT, d-DTBT, and t-DTBT (reproduced with permission from ref. 95. Copyright 2022, Wiley-VCH GmbH).

and their corresponding dioxide derivatives M-C_2H_5 (CS–CH_3 and CS–C_2H_5) were selected to be guest and host, respectively (Fig. 10a). The M-CH_3 and M-C_2H_5 nanocrystals were further applied in *in vivo* imaging. Fetal bovine serum was chosen as the aqueous medium for M-CH_3 and M-C_2H_5 nanocrystals which was irradiated by a 365 nm handheld UV lamp for 30 s before being injected into Balb/c nude mice to realize phosphorescence imaging. The signal-to-background ratios (SBRs) of subcutaneous phosphorescence imaging with M-CH_3 and M-C_2H_5 nanocrystals reached 310 and 147, respectively. The pre-excitation ability prevented the harm of UV light to the living body. Besides, the application of nanocrystals in *in vivo* cancer diagnosis was studied and the high-contrast labeling of tumors in living mice was realized.

In the same year, Cai *et al.* fabricated a fused-ring host–guest material with 5-phenyl-10,11-dihydro-5*H*-diindeno[1,2-*b*:2′,1′-d]pyrrole (PDPy) as the guest molecule and triphenylamine (TPA) as the host molecule, which led to long-wavelength phosphorescence emission at 607 nm with a long lifetime of 274 ms (Fig. 10b).[92] A top-down method was employed using PDPy/TPA to obtain water-soluble nanoparticles with the amphiphilic polymer F127 as the encapsulation matrix, and the nanoparticles were applied in bioimaging. PDPy/TPA NPs were used in HeLa cells to realize dual-channel bioimaging and the red (600–680 nm) emission channel was assigned to be phosphorescence. The time-resolved luminescence imaging in cells implied that the red

phosphorescent signal was still intense after 120 μs; in addition, the phosphorescence time-resolved imaging *in vivo* also showed the phosphorescent signal after the removal of light excitation for 7.5 min with SBRs of 21.58.

In 2022, Ding *et al.* constructed ultralong-lifetime near-infrared organic small molecular phosphorescence materials through the guest–host doped strategy and applied them in tumor imaging in living mice.[93] A series of pyrene derivatives with high conjugation were selected as guest molecules and the host benzophenone (BPO) functioned from two aspects, assisting transfers and suppressing the nonradiative transition of guest excitons (Fig. 10c). Among these obtained materials, DMAPy/BPO was chosen to be encapsulated by the biocompatible amphiphilic copolymer F127 to acquire nanoparticles due to it having the longest wavelength and a quite long lifetime. The SBRs of DMAPy/BPO NPs in subcutaneous and armpit tumor phosphorescence imaging at 10 s reached 160 and 43, respectively.

In addition to the guest–host doped system, a single molecular system has been revealed and utilized in bioimaging too. In 2021, Zhang *et al.* synthesized two kinds of single molecular RTP materials combining molecule engineering and AIE.[94] The two compounds phenyl-(2,3,4,5-tetraphenyl-1*H*-pyrrol-1-yl)methanone (TPM) and (4-chlorophenyl)-(2,3,4,5-tetraphenyl-1*H*-pyrrol-1-yl) methanone (TPM-Cl) introduced an aromatic carbonyl group based on tetraphenylpyrrole (TePP) to initiate spin–orbital coupling and enhance ISC, leading to phosphorescent emission when forming AIEgens (Fig. 10d). TPM and TPM-Cl could form stable nanoparticles possessing two-photon absorption characteristic at 80% water content with long lifetimes of 18.5 μs and 7.4 μs, respectively, which were suitable for bioimaging. Subsequently, TPM-based nanoparticles were applied in HeLa cells to demonstrate the biological imaging ability, and the results indicated that TPM-based nanoparticles emitted bright phosphorescence when irradiated with an 800 nm laser, proving the two-photon biological imaging ability. The nanoparticles also displayed time-resolved cell imaging capability with clear phosphorescence signals after 100 μs; besides, the afterglow imaging was realized in mice with SBRs reaching 7.14 ± 0.65.

In 2022, Li and coworkers developed RTP materials on the basis of single molecules possessing long-wavelength excitation and phosphorescent emission simultaneously.[95] Sunlight and a mobile phone flashlight as safe light sources were employed to realize red afterglow imaging of lymph nodes in living mice. Three luminogens (DTBT) were synthesized consisting of electron donor triphenylamine and acceptor benzothiadiazole with different geometries and numbers through the Suzuki reactions (Fig. 10e), the coated water-soluble nanoparticles of which were obtained with F127 as the encapsulating body. These nanoparticles could still achieve red phosphorescent emission in the region of 630–660 nm with an obvious absorption band in the visible region of 400–600 nm, but lifetimes decreased from the millisecond level to the microsecond level, while the afterglow signals lasted a long time with 1 h for s-DTBT, 20 min for d-DTBT, and 2 min for t-DTBT, making them suitable for afterglow imaging. Irradiated by sunlight, the s-DTBT nanoparticles achieved high SBRs of 191 and 169 for imaging subcutaneous tissue and axillary lymph nodes of living mice, respectively, and 230 and 17 when excited with a mobile phone flashlight.

5 Summary and outlook

To conclude, organic room-temperature phosphorescent materials constructed by various strategies show different luminescent properties and have been applied in different fields. These differences in RTP emission properties including wavelength, lifetime, and quantum yield mean that RTP materials exhibit huge application value, and aimed at different fields the need for RTP performance is diverse. Therefore, this review mainly summarized the recent progress with organic RTP materials with diversified properties towards application, and it was found that the development direction of RTP materials towards application is specific to a certain extent. Though great progress has been made with these pure organic RTP materials in diverse fields, there is still a huge research space to fabricate even better applied RTP materials. To obtain efficient organic light-emitting diodes, phosphorescent materials need to meet the characteristics of high quantum yield and short lifetime, while RTP materials for anti-counterfeiting and encryption applications often require rich luminous colors and to perform differently under UV excitation. Application in biological imaging demands phosphorescent materials to have longer wavelengths and longer lifetimes to eliminate fluorescence background interference and gain higher signal-to-noise ratios. Moreover, the application scope should be broadened due to the extraordinary optical properties of RTP materials. Although there are various strategies to regulate the luminescent behaviors of RTP materials by enhancing the ISC process and suppressing nonradiative deactivation, the detailed mechanism of some systems is still ambiguous. The deep development of organic RTP materials will not only improve the application value, but is also significant to the development of the photochemical mechanism. Therefore, although it is challenging to carry out deep studies into the RTP luminescence mechanism, further exploration for RTP materials will be helpful for understanding photoluminescence deeply and promoting the practical application of photoelectric functional materials in our lives.

Conflicts of interest

The authors declare no conflict of interest.

Acknowledgements

We gratefully acknowledge the financial support from the National Key Research and Development Program of China (2022YFB3203500), the National Natural Science Foundation of China (21788102, 22125803, and 22020102006), project support

by the Shanghai Municipal Science and Technology Major Project (Grant No. 2018SHZDZX03), Program of Shanghai Academic/Technology Research Leader (20XD1421300), and the Fundamental Research Funds for the Central Universities. The authors thank Dr. B. Ding and Y. Zhao for helpful discussions.

References

1 T. Zhang, X. Ma, H. Wu, L. Zhu, Y. Zhao and H. Tian, Molecular engineering for metal-free amorphous materials with room-temperature phosphorescence, *Angew. Chem., Int. Ed.*, 2020, **59**, 11206–11216.
2 X. Yang and D. Yan, Long-afterglow metal-organic frameworks: reversible guest-induced phosphorescence tunability, *Chem. Sci.*, 2016, **7**, 4519–4526.
3 X.-G. Yang, Z.-M. Zhai, X.-M. Lu, J.-H. Qin, F.-F. Li and L.-F. Ma, Hexanuclear Zn(II)-induced dense π-stacking in a metal-organic framework featuring long-lasting room temperature phosphorescence, *Inorg. Chem.*, 2020, **59**, 10395–10399.
4 P. Pinter, R. Pittkowski, J. Soellner and T. Strassner, The chameleonic nature of platinum(ii) imidazopyridine complexes, *Chem. – Eur. J.*, 2017, **23**, 14173.
5 J.-A. Li, J. Zhou, Z. Mao, Z. Xie, Z. Yang, B. Xu, C. Liu, X. Chen, D. Ren, H. Pan, G. Shi, Y. Zhang and Z. Chi, *Angew. Chem., Int. Ed.*, 2018, **57**, 6449.
6 X. Ma, C. Xu, J. Wang and H. Tian, Amorphous pure organic polymers for heavy-atom-free efficient room-temperature phosphorescence emission, *Angew. Chem., Int. Ed.*, 2018, **57**, 10854.
7 F. Gu, B. Ding, X. Ma and H. Tian, Tunable fluorescence and room-temperature phosphorescence from multiresponsive pure organic copolymers, *Ind. Eng. Chem. Res.*, 2020, **59**, 1578–1583.
8 C. Zhao, Y. Jin, J. Wang, X. Cao, X. Ma and H. Tian, Heavy-atom-free amorphous materials with facile preparation and efficient room-temperature phosphorescence emission, *Chem. Commun.*, 2019, **55**, 5355–5358.
9 Z. An, C. Zheng, Y. Tao, R. Chen, H. Shi, T. Chen, Z. Wang, H. Li, R. Deng, X. Liu and W. Huang, Stabilizing triplet excited states for ultralong organic phosphorescence, *Nat. Mater.*, 2015, **14**, 685–690.
10 J. Wang, X. Gu, H. Ma, Q. Peng, X. Huang, X. Zheng, S. H. P. Sung, G. Shan, J. W. Y. Lam, Z. Shuai and B. Z. Tang, A facile strategy for realizing room temperature phosphorescence and single molecule white light emission, *Nat. Commun.*, 2018, **9**, 2963.
11 Q. Xu, L. Ma, S. Sun and X. Ma, Achieving visible-light-excited organic room-temperature phosphorescence by manipulating p–π conjugation, *J. Mater. Chem. C*, 2021, **9**, 14623–14627.
12 C. K. Chen and B. Liu, Enhancing the performance of pure organic room-temperature phosphorescent luminophores, *Nat. Commun.*, 2019, **10**, 2111.
13 W. Z. Yuan, X. Y. Shen, H. Zhao, J. W. Y. Lam, L. Tang, P. Lu, C. Wang, Y. Liu, Z. Wang, Q. Zheng, J. Z. Sun, Y. Ma and B. Z. Tang, Crystallization-induced phosphorescence of pure organic luminogens at room temperature, *J. Phys. Chem. C*, 2010, **114**, 6090–6099.
14 H. Liu, Z. Bian, Q. Cheng, L. Lian, Y. Wang and H. Zhang, Controllably realizing elastic/plastic bending based on a room-temperature phosphorescent waveguiding organic crystal, *Chem. Sci.*, 2019, **10**, 227–232.
15 S. Jena, J. Eyyathiyil, S. K. Behera, M. Kitahara, Y. Imai and P. Thilagar, Crystallization induced room-temperature phosphorescence and chiral photoluminescence properties of phosphoramides, *Chem. Sci.*, 2022, **13**, 5893–5901.
16 Y. Zhao, L. Ma, Z. Huang, J. Zhang, I. Willner, X. Ma and H. Tian, Visible light activated organic room-temperature phosphorescence based on triplet-to-singlet Förster-resonance energy transfer, *Adv. Opt. Mater.*, 2022, **10**, 2102701.
17 H. Gui, Z. Huang, Z. Yuan and X. Ma, Ambient white-light afterglow emission based on triplet-to-singlet Förster resonance energy transfer, *CCS Chem.*, 2022, **4**, 173–181.
18 T. Wang, Z. Tang, D. Xu, W. Sun, Y. Deng, Q. Wang, X. Zhang, P. Su and G. Zhang, Waterborne polyacrylates with thermally activated delayed fluorescence and two-state phosphorescence, *Mater. Chem. Front.*, 2018, **2**, 559–565.
19 B. Wu, X. Xu, Y. Tang, X. Han and G. Wang, Multifunctional optical polymeric films with photochromic, fluorescent, and ultra-long room temperature phosphorescent properties, *Adv. Opt. Mater.*, 2021, **9**, 2101266.
20 B. Ding, H. Gao, C. Wang and X. Ma, Multifunctional optical polymeric films with photochromic, fluorescent, and ultra-long room temperature phosphorescent properties, *Chem. Commun.*, 2021, **57**, 3154–3157.
21 T. Zhang, X. Ma and H. Tian, A facile way to obtain near-infrared room-temperature phosphorescent soft materials based on Bodipy dyes, *Chem. Sci.*, 2020, **11**, 482–487.
22 C. Xu, C. Yin, W. Wu and X. Ma, Tunable room-temperature phosphorescence and circularly polarized luminescence encoding helical supramolecular polymer, *Sci. China: Chem.*, 2022, **65**, 75–81.
23 Z.-Y. Zhang, Y. Chen and Y. Liu, Efficient room-temperature phosphorescence of a solid-state supramolecule enhanced by cucurbit[6]uril, *Angew. Chem., Int. Ed.*, 2019, **58**, 6028.
24 S. Garain, B. C. Garain, M. Eswaramoorthy, S. K. Pati and S. J. George, Light-harvesting supramolecular phosphors: Highly efficient room temperature phosphorescence in solution and hydrogels, *Angew. Chem., Int. Ed.*, 2021, **60**, 19720.
25 M. Liu, C. Zheng, Y. Zheng, X. Wu and J. Shen, Binding model-tuned room-temperature phosphorescence of the bromo-naphthol derivatives based on cyclodextrins, *RSC Adv.*, 2022, **12**, 19313–19316.
26 C. Xu, X. Lin, W. Wu and X. Ma, Room-temperature phosphorescence of a water-soluble supramolecular organic framework, *Chem. Commun.*, 2021, **57**, 10178–10181.
27 L. Ma, Q. Xu, S. Sun, B. Ding, Z. Huang, X. Ma and H. Tian, A universal strategy for tunable persistent luminescent materials via radiative energy transfer, *Angew. Chem., Int. Ed.*, 2022, **61**, e202115748.

28 J. Cao, M. Zhang, M. Singh, Z. An, L. Ji, H. Shi and Y. Jiang, Highly efficient heavy atom free room temperature phosphorescence by host-guest doping, *Front. Chem.*, 2021, **9**, 781294.
29 M. Li, X. Cai, Z. Chen, K. Liu, W. Qiu, W. Xie, L. Wang and S.-J. Su, Boosting purely organic room-temperature phosphorescence performance through a host–guest strategy, *Chem. Sci.*, 2021, **12**, 13580–13587.
30 Y. Zhao, B. Ding, Z. Huang and X. Ma, Highly efficient organic long persistent luminescence based on host–guest doping systems, *Chem. Sci.*, 2022, **13**, 8412–8416.
31 Y. He, N. Cheng, X. Xu, J. Fu and J. Wang, A high efficiency pure organic room temperature phosphorescence polymer PPV derivative for OLED, *Org. Electron.*, 2019, **64**, 247–251.
32 G. Zhan, Z. Liu, Z. Q. Bian and C. Huang, Recent advances in organic light-emitting diodes based on pure organic room temperature phosphorescence materials, *Front. Chem.*, 2019, **7**, 305.
33 A. Krishna, V. Darshana, C. H. Suresha, K. N. N. Unnia and R. L. Varma, Solution processable carbazole derivatives for dopant free single molecule white electroluminescence by room temperature phosphorescence, *J. Photochem. Photobiol., A*, 2018, **360**, 249–254.
34 A. Tomkeviciene, T. Matulaitis, M. Guzauskas, V. Andruleviciene, D. Volyniuk and J. V. Grazulevicius, Thianthrene and acridan-substituted benzophenone or diphenylsulfone: Effect of triplet harvesting via TADF and phosphorescence on efficiency of all-organic OLEDS, *Org. Electron.*, 2019, **70**, 227–239.
35 H. Chen, Y. Deng, X. Zhu, L. Wang, L. Lv, X. Wu, Z. Li, Q. Shi, A. Peng, Q. Peng, Z. Shuai, Z. Zhao, H. Chen and H. Huang, Toward achieving single-molecule white electroluminescence from dual emission of fluorescence and phosphorescence, *Chem. Mater.*, 2020, **32**, 4038–4044.
36 G. Bergamini, A. Fermi, C. Botta, U. Giovanella, S. D. Motta, F. Negri, R. Peresutti, M. Gingras and P. Ceroni, A persulfurated benzene molecule exhibits outstanding phosphorescence in rigid environments: From computational study to organic nanocrystals and OLED applications, *J. Mater. Chem. C*, 2013, **1**, 2717–2724.
37 T. Wang, X. Su, X. Zhang, X. Nie, L. Huang, X. Zhang, X. Sun, Y. Luo and G. Zhang, Aggregation-induced dual-phosphorescence from organic molecules for nondoped light-emitting diodes, *Adv. Mater.*, 2019, **31**, 1904273.
38 X. Liu, L. Yang, X. Li, L. Zhao, S. Wang, Z.-H. Lu, J. Ding and L. Wang, An electroactive pure organic room-temperature phosphorescence polymer based on a donor-oxygen-acceptor geometry, *Angew. Chem., Int. Ed.*, 2021, **60**, 2455–2463.
39 H. F. Higginbotham, M. Okazaki, P. Silva, S. Minakata, Y. Takeda and P. Data, Heavy-atom-free room-temperature phosphorescent organic light-emitting diodes enabled by excited states engineering, *ACS Appl. Mater. Interfaces*, 2021, **13**, 2899–2907.
40 J. Wang, B. Liang, J. Wei, Z. Li, Y. Xu, T. Yang, C. Li and Y. Wang, Highly efficient electrofluorescence material based on pure organic phosphor sensitization, *Angew. Chem., Int. Ed.*, 2021, **60**, 15335–15339.
41 X. Han, X. Wang, Y. Wu, J. Zhao, Y. Liu, H. Shu, X. Wu, H. Tong and L. Wang, Modulation of triplet-mediated emission from selenoxanthen-9-one-based D-A-D type emitters through tuning the twist angle to realize electroluminescence efficiency over 25%, *J. Mater. Chem. C*, 2022, **10**, 7437.
42 X. Ma, C. Xu, J. Wang and H. Tian, Amorphous pure organic polymers for heavy-atom-free efficient room-temperature phosphorescence emission, *Angew. Chem., Int. Ed.*, 2018, **57**, 10854–10858.
43 R. Gao, D. Yan, D. G. Evans and X. Duan, Layer-by-layer assembly of long-afterglow self-supporting thin films with dual-stimuli-responsive phosphorescence and antiforgery applications, *Nano Res.*, 2017, **10**, 3606–3617.
44 W.-L. Zhou, W. Lin, Y. Chen, X.-Y. Dai, Zh. Liu and Y. Liu, Layer-by-layer assembly of long-afterglow self-supporting thin films with dual-stimuli-responsive phosphorescence and antiforgery applications, *Chem. Sci.*, 2022, **13**, 573.
45 R. Liu, T. Jiang, D. Liu and X. Ma, A facile and green strategy to obtain organic room-temperature phosphorescence from natural lignin, *Sci. China: Chem.*, 2022, **65**, 1100–1104.
46 B. Zhou, Z. Qi and D. Yan, Highly efficient and direct ultralong all-phosphorescence from metal-organic framework photonic glasses, *Angew. Chem., Int. Ed.*, 2022, **61**, e202208735.
47 Z. Yuan, L. Zou, D. Chang and X. Ma, Conformation-dependent phosphorescence of galactose-decorated phosphors and assembling-induced phosphorescence enhancement, *ACS Appl. Mater. Interfaces*, 2020, **12**, 52059–52069.
48 G. Jiang, Q. Li, A. Lv, L. Liu, J. Gong, H. Ma, J. Wang and B. Z. Tang, Modulation of the intramolecular hydrogen bonding and push-pull electron effects toward realizing highly efficient organic room temperature phosphorescence, *J. Mater. Chem. C*, 2022, **10**, 13797–13804.
49 X. Han, K. Chen, Y. Lei, J. Huang, S. Wei, Z. Cai, H. Wu, M. Liu, X. Huang and Y. Dong, Dual guests synergistically tune the phosphorescence properties of doped systems through chemical interactions with bases, *ACS Mater. Lett.*, 2022, **4**, 1764–1773.
50 F. Nie, B. Zhou, K.-Z. Wang and D. Yan, Highly tunable ultralong room-temperature phosphorescence from ionic supramolecular adhesives for multifunctional applications, *Chem. Eng. J.*, 2022, **430**, 133084.
51 Z. Yin, M. Gu, H. Ma, X. Jiang, J. Zhi, Y. Wang, H. Yang, W. Zhu and Z. An, Molecular engineering through control of structural deformation for highly efficient ultralong organic phosphorescence, *Angew. Chem., Int. Ed.*, 2021, **60**, 2058–2063.
52 Y. Ning, J. Yang, H. Si, H. Wu, X. Zheng, A. Qin and B. Z. Tang, Ultralong organic room-temperature phosphorescence of electron-donating and commercially available host and guest molecules through efficient Förster resonance energy transfer, *Sci. China: Chem.*, 2021, **64**, 739–744.

53 H. Gao, B. Ding, C. Wang and X. Ma, Synergetic enhancement of room-temperature phosphorescence via water molecules as a hydrogen bonding bridge, *J. Mater. Chem. C*, 2021, **9**, 16581.
54 Y. Tian, J. Yang, Z. Liu, M. Gao, X. Li, W. Che, M. Fang and Z. Li, Multistage stimulus-responsive room temperature phosphorescence based on host-guest doping systems, *Angew. Chem., Int. Ed.*, 2021, **60**, 20259–20263.
55 R. Liu, B. Ding, D. Liu and X. Ma, Switchable circularly polarized room-temperature phosphorescence based on pure organic amorphous binaphthyl polymer, *Chem. Eng. J.*, 2021, **421**, 129732.
56 Z. Huang, Z. He, B. Ding, H. Tian and X. Ma, Switchable circularly polarized Room-Temperature phosphorescence based on pure organic amorphous binaphthyl polymer, *Nat. Commun.*, 2022, **13**, 7841.
57 P. She, Y. Yu, Y. Qin, Y. Zhang, F. Li, Y. Ma, S. Liu, W. Huang and Q. Zhao, Controlling organic room temperature phosphorescence through external heavy-atom effect for white light emission and luminescence printing, *Adv. Opt. Mater.*, 2020, **8**, 1901437.
58 J. Ren, Y. Wang, Y. Tian, Z. Liu, X. Xiao, J. Yang, M. Fang and Z. Li, Force-Induced turn-on persistent room-temperature phosphorescence in purely organic luminogen, *Angew. Chem., Int. Ed.*, 2021, **60**, 12335–12340.
59 Q. Li and Z. Li, Molecular packing: Another key point for the performance of organic and polymeric optoelectronic materials, *Acc. Chem. Res.*, 2020, **53**, 962–973.
60 A. Huang, Q. Li and Z. Li, Molecular uniting set identified characteristic (MUSIC) of organic optoelectronic material, *Chin. J. Chem.*, 2022, **40**, 2356–2370.
61 T. Zhang, C. Wang and X. Ma, Metal-free room-temperature phosphorescent systems for pure white-light emission and latent fingerprint visualization, *Ind. Eng. Chem. Res.*, 2019, **58**, 7778–7785.
62 D. Li, Y. Yang, J. Yang, M. Fang, B. Z. Tang and Z. Li, Completely aqueous processable stimulus responsive organic room temperature phosphorescence materials with tunable afterglow color, *Nat. Commun.*, 2022, **13**, 347.
63 J. Yang, M. Fang and Z. Li, Stimulus-responsive room temperature phosphorescence materials: Internal mechanism, design strategy, and potential application, *Acc. Mater. Res.*, 2021, **2**, 644–654.
64 F. Li, L. Tang, Y. Liu and J. Shao, Background-free latent fingerprint imaging based on carbonized polymers@silica powder with intense green room-temperature phosphorescence, *Opt. Mater.*, 2022, **128**, 112356.
65 J. Yao, J. Kong, L. Kong, X. Wang, W. Shi and C. Lu, The phosphorescence nanocomposite thin film with rich oxygen vacancy: Towards sensitive oxygen sensor, *Chin. Chem. Lett.*, 2022, **33**, 3977–3980.
66 B. Zhou and D. Yan, Stimuli-responsive organic phosphorescence through energy transfer, *Sci. China: Chem.*, 2021, **64**, 509–510.
67 E. G. Ermolina, R. T. Kuznetsova, Y. V. Aksenova, R. M. Gadirova, T. N. Kopylova, E. V. Antina, M. B. Berezin and A. S. Semeikin, Novel quenchometric oxygen sensing material based on diiodine-substituted boron dipyrromethene dye, *Sens. Actuators, B*, 2014, **197**, 206–210.
68 S. Wang, Z. Cheng, X. Han, H. Shu, X. Wu, H. Tong and L. Wang, Efficient and tunable purely organic room temperature phosphorescence films from selenium-containing emitters achieved by structural isomerism, *J. Mater. Chem. C*, 2022, **10**, 5141.
69 Y. Zhou, W. Qin, C. Du, H. Gao, F. Zhu and G. Liang, Long-lived room-temperature phosphorescence for visual and quantitative detection of oxygen, *Angew. Chem., Int. Ed.*, 2019, **58**, 12102–12106.
70 W.-J. Guo, Y.-Z. Chen, C.-H. Tung and L.-Z. Wu, Ultralong room-temperature phosphorescence of silicon-based pure organic crystal for oxygen sensing, *CCS Chem.*, 2022, **4**, 1007–1015.
71 S. Sun, J. Wang, L. Ma, X. Ma and H. Tian, A universal strategy for organic fluid phosphorescence materials, *Angew. Chem., Int. Ed.*, 2021, **60**, 18557–18560.
72 X. Luo, L. Chen, B. Liu, Z. Yang, L. Wei, Z. Yuan, Y. Wen, Y. Mu, Y. Huo, H.-L. Zhang and S. Ji, Water-enhanced high-efficiency persistent room-temperature phosphorescence materials for temperature sensing via crystalline transformation, *J. Mater. Chem. C*, 2022, **10**, 13210–13216.
73 Y. Zhang, X. Chen, J. Xu, Q. Zhang, L. Gao, Z. Wang, L. Qu, K. Wang, Y. Li, Z. Cai, Y. Zhao and C. Yang, Cross-linked polyphosphazene nanospheres boosting long-lived organic room-temperature phosphorescence, *J. Am. Chem. Soc.*, 2022, **144**, 6107–6117.
74 V. Ntziachristos, J. Ripoll, L. V. Wang and R. Weissleder, Looking and listening to light: The evolution of whole-body photonic imaging, *Nat. Biotechnol.*, 2005, **23**, 313–320.
75 X. Zhen, Y. Tao, Z. An, P. Chen, C. Xu, R. Chen, W. Huang and K. Pu, Ultralong phosphorescence of water-soluble organic nanoparticles for in vivo afterglow imaging, *Adv. Mater.*, 2017, **29**, 1606665.
76 L. Wang, Q. Xia, M. Hou, C. Yan, Y. Xu, J. Qu and R. Liu, A photostable cationic fluorophore for long-term bioimaging, *J. Mater. Chem. B*, 2017, **5**, 9183.
77 M. Yu, W. Zhao, F. Ni, Q. Zhao and C. Yang, Photoswitchable thermally activated delayed fluorescence nanoparticles for "Double-Check" confocal and time-resolved luminescence bioimaging, *Adv. Opt. Mater.*, 2022, **10**, 2102437.
78 H.-J. Yu, Q. Zhou, X. Dai, F.-F. Shen, Y.-M. Zhang, X. Xu and Y. Liu, Photooxidation-driven purely organic room-temperature phosphorescent lysosome-targeted imaging, *J. Am. Chem. Soc.*, 2021, **143**, 13887–13894.
79 Y. Zeng, V. P. Nguyen, Y. Li, D. H. Kang, Y. M. Paulus and J. Kim, Chorioretinal hypoxia detection using lipid-polymer hybrid organic room-temperature phosphorescent nanoparticles, *ACS Appl. Mater. Interfaces*, 2022, **14**, 18182–18193.
80 X. Yu, W. Liang, Q. Huang, W. Wu, J. J. Chruma and C. Yang, Room-temperature phosphorescent γ-cyclodextrin-cucurbit[6]uril-cowheeled [4]rotaxanes for specific sensing of tryptophan, *Chem. Commun.*, 2019, **55**, 3156.

81 J. Wang, Z. Huang, X. Ma and H. Tian, Visible-light-excited room-temperature phosphorescence in water by cucurbit[8] uril-mediated supramolecular assembly, *Angew. Chem., Int. Ed.*, 2020, **59**, 9928–9933.
82 W.-L. Zhou, Y. Chen, Q. Yu, H. Zhang, Z.-X. Liu, X.-Y. Dai, J.-J. Li and Y. Liu, Ultralong purely organic aqueous phosphorescence supramolecular polymer for targeted tumor cell imaging, *Nat. Commun.*, 2020, **11**, 4655.
83 C. Wang, Y.-H. Liu and Y. Liu, Near-infrared phosphorescent switch of diarylethene phenylpyridinium derivative and cucurbit[8]uril for cell imaging, *Small*, 2022, **18**, 2201821.
84 X.-K. Ma, X. Zhou, J. Wu, F.-F. Shen and Y. Liu, Two-photon excited near-infrared phosphorescence based on secondary supramolecular confinement, *Adv. Sci.*, 2022, **9**, 2201182.
85 F.-F. Shen, Z. Liu, H.-J. Yu, H. Wang, X. Xu and Y. Liu, Macrocyclic confined purely organic room-temperature phosphorescence three-photon targeted imaging, *Adv. Opt. Mater.*, 2022, **10**, 2200245.
86 X.-Y. Dai, M. Huo, X. Dong, Y.-Y. Hu and Y. Liu, Noncovalent polymerization-activated ultrastrong near-infrared room-temperature phosphorescence energy transfer assembly in aqueous solution, *Adv. Mater.*, 2022, **34**, 2203534.
87 J. Song, L. Ma, S. Sun, H. Tian and X. Ma, Reversible multilevel stimuli-responsiveness and multicolor room-temperature phosphorescence emission based on a single-component system, *Angew. Chem., Int. Ed.*, 2022, **61**, e202206157.
88 T. Zhu, T. Yang, Q. Zhang and W. Z. Yuan, Clustering and halogen effects enabled red/near-infrared room temperature phosphorescence from aliphatic cyclic imides, *Nat. Commun.*, 2022, **13**, 2658.
89 X. Zheng, Y. Huang, D. Xiao, S. Yang, Z. Lin and Q. Ling, Space conjugation induced white light and room-temperature phosphorescence from simple organic small molecules: Single-component WLED driven by both UV and blue chips, *Mater. Chem. Front.*, 2021, **5**, 6960–6968.
90 X. Zhen, Y. Tao, Z. An, P. Chen, C. Xu, R. Chen, W. Huang and K. Pu, Ultralong Phosphorescence of water-soluble organic nanoparticles for in vivo afterglow imaging, *Adv. Mater.*, 2017, **29**, 1606665.
91 Y. Wang, H. Gao, J. Yang, M. Fang, D. Ding, B. Z. Tang and Z. Li, High performance of simple organic phosphorescence host-guest materials and their application in time-resolved bioimaging, *Adv. Mater.*, 2021, **33**, 2007811.
92 W. Dai, Y. Zhang, X. Wu, S. Guo, J. Ma, J. Shi, B. Tong, Z. Cai, H. Xie and Y. Dong, Red-emissive organic room-temperature phosphorescence material for time-resolved luminescence bioimaging, *CCS Chem.*, 2022, **4**, 2550–2559.
93 F. Xiao, H. Gao, Y. Lei, W. Dai, M. Liu, X. Zheng, Z. Cai, X. Huang, H. Wu and D. Ding, Guest-host doped strategy for constructing ultralong-lifetime near-infrared organic phosphorescence materials for bioimaging, *Nat. Commun.*, 2022, **13**, 186.
94 J. Yang, Y. Zhang, X. Wu, W. Dai, D. Chen, J. Shi, B. Tong, Q. Peng, H. Xie, Z. Cai, Y. Dong and X. Zhang, Rational design of pyrrole derivatives with aggregation-induced phosphorescence characteristics for time-resolved and two-photon luminescence imaging, *Nat. Commun.*, 2021, **12**, 4883.
95 Y. Fan, S. Liu, M. Wu, L. Xiao, Y. Fan, M. Han, K. Chang, Y. Zhang, X. Zhen, Q. Li and Z. Li, Mobile phone flashlight-excited red afterglow bioimaging, *Adv. Mater.*, 2022, **34**, 2201280.